

Electronic Supplementary Information

Two structurally new Lindqvist hexaniobate-templated silver thiolate clusters

Zichen Zhao,^a Mengyun Zhao,^a Lan Deng,*^a Qing Li,^a Jing Zhang,^a Haifeng Su,^b Hongjin Lv,*^a Guo-Yu Yang^a

^a MOE Key Laboratory of Cluster Science, Beijing Key Laboratory of Photoelectric/Electrophotonic Conversion Materials, School of Chemistry and Chemical Engineering, Beijing Institute of Technology, Beijing 102488, P. R. China.

^b College of Chemistry and Chemical Engineering, Xiamen University, Xiamen 361005, People's Republic of China

Corresponding author E-mail: hlv@bit.edu.cn; landeng@bit.edu.cn

Table of contents

1. Experimental details.....	S3
2. Single-crystal X-ray crystallography.....	S4
3. Bond valence sum (BVS) calculation.....	S5
4. Fig. S1 The digital photographs of Ag ₄₅ and Ag ₄₁ crystals.....	S5
5. Fig. S2 ORTEP representation of the Ag ₄₅ cluster.....	S6
6. Fig. S3 ORTEP representation of the Ag ₄₁ cluster.....	S6
7. Fig. S4 Experimental and simulated PXRD patterns of Ag ₄₅ and Ag ₄₁ clusters.....	S7
8. Fig. S5 The coordination modes of [Nb ₆ O ₁₉] ⁸⁻ anion towards silver atoms.....	S7
9. Fig. S6 FT-IR spectra of TBA-Nb ₆ , Ag ₄₅ , and Ag ₄₁ clusters.....	S8

10. Fig. S7 XPS data of Ag₄₅ cluster.....	S8
11. Fig. S8 XPS data of Ag₄₁ cluster.....	S9
12. Fig. S9 Positive-ion ESI-MS spectra of the clusters of Ag₄₅ dissolved in CH ₃ OH.....	S9
13. Fig. S10 Positive-ion ESI-MS spectra of the clusters of Ag₄₁ dissolved in CH ₃ OH.....	S10
14. Fig. S11 The coordination modes of 23 ⁱ PrS ⁻ ligands towards silver atoms in Ag₄₅ cluster.....	S10
15. Fig. S12 The coordination modes of 14 CH ₃ COO ⁻ ligands towards silver atoms in Ag₄₅ cluster.....	S11
16. Fig. S13 The coordination modes of 24 ⁱ PrS ⁻ ligands towards silver atoms in Ag₄₁ cluster.....	S11
17. Fig. S14 The coordination modes of 5 CH ₃ COO ⁻ ligands towards silver atoms in Ag₄₁ cluster.....	S12
18. Fig. S15 The coordination modes of S atoms in Ag₄₁ cluster.....	S12
19. Fig. S16 Packing structure of Ag₄₅ cluster in the <i>bc</i> plane.....	S13
20. Fig. S17 Packing structure of Ag₄₁ cluster.....	S13
21. Fig. S18 One-dimensional chain structure of Ag₄₁ cluster.....	S14
22. Fig. S19 The solid-state UV-vis spectra of Ag₄₅ and Ag₄₁ clusters.....	S14
23. Fig. S20 Photothermal conversion of Ag₄₅ and Ag₄₁ clusters under 532 nm laser irradiation.....	S15
24. Fig. S21 FT-IR spectra of (a) Ag₄₅ and (b) Ag₄₁ clusters before and after photothermal tests.....	S15
25. Fig. S22 TGA curves of Ag₄₅ at a scanning rate of 10 °C/ min under N ₂ atmosphere.....	S16
26. Fig. S23 FT-IR spectra of Ag₄₁ clusters before and after heating 80 °C.....	S16
27. Table S1 Crystal data and structure refinements for Ag₄₅ and Ag₄₁	S17
28. Table S2 Selected bond distances (Å) for Ag₄₅	S18
29. Table S3 Selected bond distances (Å) for Ag₄₁	S20
30. Table S4 BVS values for Nb atoms of Ag₄₅	S22
31. Table S5 BVS values for Nb atoms of Ag₄₁	S22
32. Table S6 PL decay lifetimes of Ag₄₅ and Ag₄₁ clusters upon excitation at 390 nm.....	S22
33. References	S23

Experimental details

Chemicals and Materials. The (*i*Pr₂Ag)_n precursor and the [(CH₃)₄N]₅[H₃Nb₆O₁₉]·20H₂O (TMA-Nb₆) PONbs were synthesized according to the relevant literatures.^{1,2} The chemicals and solvents used in the syntheses were purchased from commercial sources and used as received without further purification. Niobium(V) oxide (Nb₂O₅) and silver acetate were purchased from Shanghai Macklin Biochemical Co., Ltd and used as received. *i*PrSH (Adamas-beta®) was purchased from Shanghai Titan Scientific Co.,Ltd and used as received. Silver acetate was purchased from Shanghai Macklin Biochemical Co., Ltd and used as received.

Characterization. The FT-IR spectra were performed on a Bruker Tensor II spectrometer using ~2 wt% KBr pellets in the range of 4000-400 cm⁻¹. UV-vis spectra were acquired on a Techcomp UV 2600 spectrophotometer at room temperature in the 200-800 nm range with optional Integration Sphere accessory. ICP-AES analyses for Ag and Nb were conducted with Spectro Arcos EOP (Axial View Inductively Coupled Plasma Spectrometer). Elemental analyses were performed on an Elementar UNICUBE. The X-ray Photoelectron Spectrum (XPS) was measured on a PHI5000 Versaprobe III. The steady-state luminescence quenching spectra was measured using Edinburgh Instruments FS5 Spectrofluorometer. The High-Resolution Electrospray Mass Spectrometry was performed on an Agilent (Santa Clara, CA, USA) ESI-TOF mass spectrometer (6224) from saturated solution of Ag₄₅ and Ag₄₁ in CH₃OH. Emission lifetime was measured with an EPL-365 picosecond pulsed diode laser system. Thermogravimetric analysis (TGA) was performed with a EXSTAR 7200 thermal analyzer at a scanning rate of 10 °C/min under N₂ atmosphere, from 30 to 800 °C. Powder XRD patterns were measured on a MiniFlex 600 diffractometer with a Cu-K α X-ray radiation source. Photothermal measurements were conducted using Laser MGL-III-532nm-300mW. The photothermal behavior of the sample was monitored by thermal imaging camera (Fotric 326C). Infrared photos and real-time temperatures were extracted from the video by FLIR tools software.

Synthesis of [Nb₆O₁₉@Ag₄₅(*i*PrS)₂₃(CH₃COO)₁₄] (Ag₄₅). (*i*Pr₂Ag)_n (0.05 mmol, 9.2 mg) and CH₃COOAg (0.1 mmol, 16.7 mg) together with TMA-Nb₆ (0.005 mmol, 8.2 mg) were dissolved in a mixed solvent of methanol: N,N'- dimethylformamide (5 mL, v/v = 1/1) under stirring at room temperature for 3 h. The reaction mixture was sealed and heated at 65 °C for 33 h, and then cooled to room temperature for 12 h. After cooling to room temperature, the light-yellow solution was filtered, and the filtrate was left for evaporation at room temperature in dark. The yellow block crystals of Ag₄₅ were crystallized after two months in ~11.5% yield (based on Ag). Elemental analysis: Calcd (%) for C₉₇H₂₀₃O₄₇S₂₃Nb₆Ag₄₅ (FW = 8270.57): Ag, 58.69; Nb, 6.74; C, 14.09; H, 2.47. Found: Ag, 57.89; Nb, 6.98; C, 14.69; H, 2.78.

Synthesis of (H₃O)₄[Nb₆O₁₉@Ag₄₁KS_{2.5}O₂(H₂O)_{7.5}(*i*PrS)₂₄(CH₃COO)₅] (Ag₄₁). The synthetic conditions were same as the procedure described for Ag₄₅, except that the reaction temperature was raised to 70 °C. After cooling to room temperature, the light-yellow solution was filtered and the filtrate left to evaporate slowly for one month in the dark at room temperature. The light red crystals of Ag₄₁ were isolated in ~9.6% yield (based on Ag). Elemental analysis: Calcd (%) for C₈₂H₂₁₀Ag₄₁KNb₆O_{42.5}S_{26.5} (FW = 7745.31): Ag, 57.10; Nb, 7.19; C, 12.71; H, 2.71. Found: Ag, 58.21; Nb, 7.23; C, 12.94; H, 2.98.

Discussion on polyoxoniobate-templated silver clusters. Currently, there are very limited reports on polyoxoniobate-templated silver clusters, which to our knowledge could be attributed to the following aspects: (1) there are limited structures of polyoxoniobates (PONbs) in comparison with those of polyoxovanadates (POVs), polyoxotungstates (POTs), and polyoxomolybdates (POMos) as mentioned by the reviewer; (2) it is extremely challenging for PONbs to produce secondary building blocks compared to that of diverse lacunary structures of POTs/POMos (e.g. lacunary Keggin- / Dawson-type structures); (3) the solubility of PONbs in organic solvents is extremely low, making it incompatible with the solubility of regular Ag chemicals used for syntheses; (4) PONbs prefer alkaline environment to remain good stability, while such alkaline environment is not friendly to common Ag(I) complexes. Therefore, the synthesis of PONb-templated silver clusters is a very difficult and challenging task.

Regarding the difference of our work from the reported PONb-templated silver clusters, there is only one relevant report by Zheng and co-workers (*Chem. Commun.*, 2023, **59**, 2927-2930.). In this work, the authors have synthesized the Nb₆-templated Ag cluster (**Ag**₃₄) using tert-butyl acetylene as a peripheral protective ligand through the solvothermal reaction of six chemicals in a ternary CH₃CN-DMF-H₂O solvent system. There are six discrete **Ag**₃₄ clusters packed together by noncovalent interactions such as van der Waals forces within one unit cell. The authors performed the ESI-MS measurement on the target **Ag**₃₄ cluster and studied its temperature-dependent emission behavior.

In contrast, we synthesized two structurally new Lindqvist hexaniobate-templated silver thiolate clusters **Ag**₄₅ and **Ag**₄₁ by using ⁱPrS⁻ and CH₃COO⁻ as surface-protecting ligands, which can further form a two-dimensional (2D) **Ag**₄₅ assembly and one-dimensional (1D) **Ag**₄₁ chain packing structures. Interestingly, the **Ag**₄₅ cluster can form a 2D packing structure, while the **Ag**₄₁ cluster can form a 1D chain through coordination bonds. Moreover, both **Ag**₄₅ and **Ag**₄₁ clusters exhibited intriguing photothermal conversion property and temperature-dependent emission behavior.

Single-crystal X-ray crystallography

The high-quality crystal of **Ag**₄₅ and **Ag**₄₁ with appropriate dimensions was chosen under an optical microscope and quickly immersed in crystal oil to prevent decomposition at both ends for data collection at 179.99 K. Crystallographic data of **Ag**₄₅ was collected on a XtaLAB Synergy R, DW system, HyPix diffractometer with Mo K α radiation (graphite monochromator, $\lambda = 0.71073 \text{ \AA}$). The structure of **Ag**₄₅ was solved with the Olex2 structure solution program using Charge Flipping,^{3,4} and refined with the XL refinement package using Least Squares minimisation.⁵ Crystallographic data of **Ag**₄₁ was collected on a Bruker APEX-II CCD diffractometer with Mo K α radiation (graphite monochromator, $\lambda = 0.71073 \text{ \AA}$). The structure of **Ag**₄₁ was solved with the Olex2 and the SHELXT structure solution program using Charge Flipping,^{3,6} and refined with the SHLXL refinement package using Least Squares minimisation.⁶ All non-hydrogen atoms were refined anisotropically, while hydrogen atoms on carbon atoms were generated geometrically and refined isotropically. A solvent mask has been used in the refinement of **Ag**₄₁ crystal, it is calculated as 59 masked electrons in a volume of 256 \AA^3 per Asymmetric Unit in **Ag**₄₁, which is consistent with the presence of 1 [H₃O]⁺, 1 [H₉O₄] (1 H₃O⁺; 3 H₂O) and 0.75 [H₂O] moieties that account for 60 electrons per Asymmetric Unit. To refine a sensible molecular model, the whole arsenal of SHELXL restraints had to be used (ISOR, DFIX, EADP, and SIMU). Some Ag atoms were refined as disordered, appropriate restraints and constraints were applied to the geometry and atomic displacement parameters of atoms in **Ag**₄₅ and **Ag**₄₁ clusters. In addition, there were two Ag/K disordered metal sites with Ag and K atoms adopting

50% occupancy in Ag_{41} cluster. Crystal structure graphics and their packing diagrams were drawn by using Diamond 4 software. Detailed crystallographic data for complexes Ag_{45} and Ag_{41} are supplemented in Table S1. CCDC 2331897 and 2347574 contain the supplementary crystallographic data for Ag_{45} and Ag_{41} , respectively. The crystallographic data can be obtained from The Cambridge Crystallographic Data Centre via www.ccdc.cam.ac.uk/data_request/cif.

Bond valence sum (BVS) calculation

The BVS values were calculated by the expression for the variation of the length r_{ab} of a bond between two atoms a and b in observed crystal with valence V_a .⁷

$$V_a = \sum \exp\left(-\frac{r_0 - r_{ab}}{B}\right)$$

where B is constant equal to 0.37 Å, r_0 is bond valence parameter for a given atom pair.

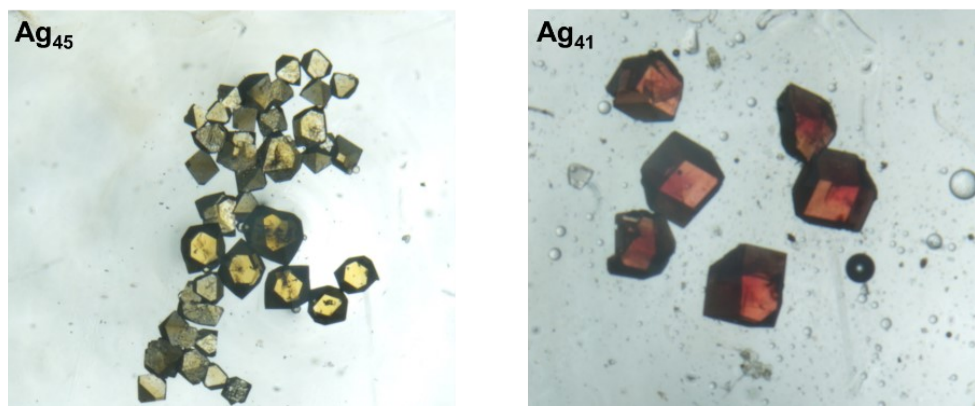


Fig. S1 The digital photographs of Ag_{45} and Ag_{41} crystals taken under the microscope.

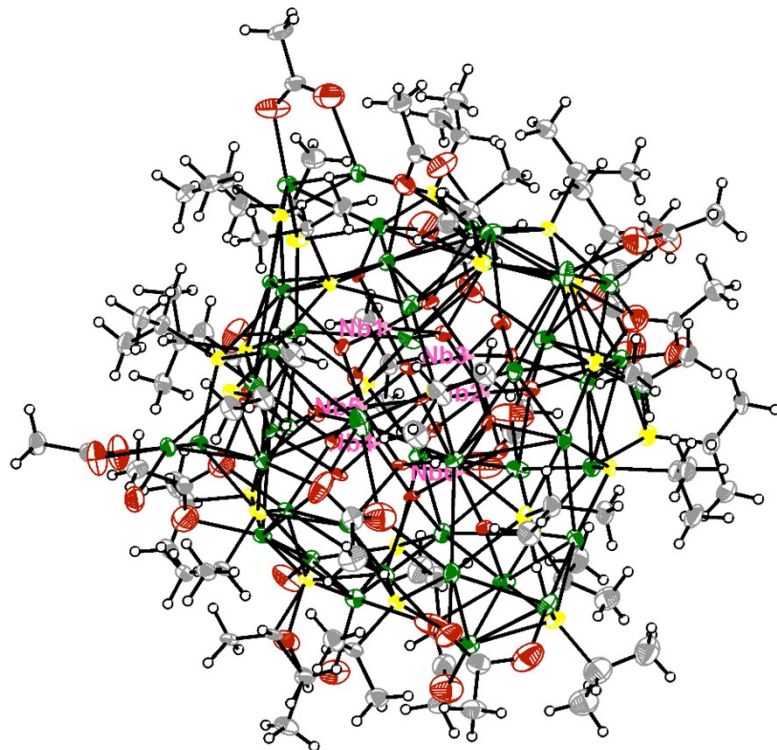


Fig. S2 A displacement ellipsoid plot of the Ag_{45} cluster. Non-H atoms are represented by ellipsoids at the 30% probability. (Color legend: green, Ag; pink, Nb; yellow, S; red, O; gray, C; white, H.)

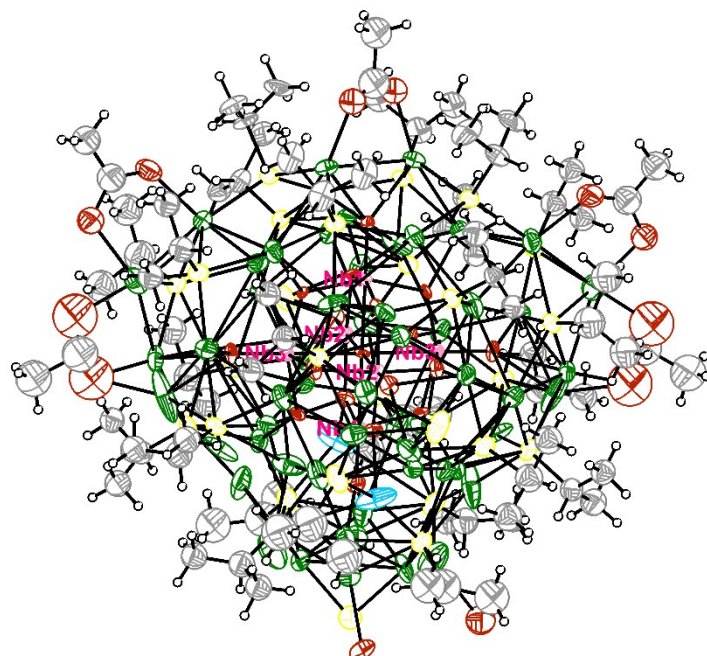


Fig. S3 A displacement ellipsoid plot of the Ag_{41} cluster. Non-H atoms are represented by ellipsoids at the 30% probability. Color codes: green, Ag; pink, Nb; yellow, S; red, O; gray, C; sky blue, Ag/K; white, H. Note: in these two disordered Ag/K atoms, both Ag29 and K1 atoms were refined as 50% occupancy.

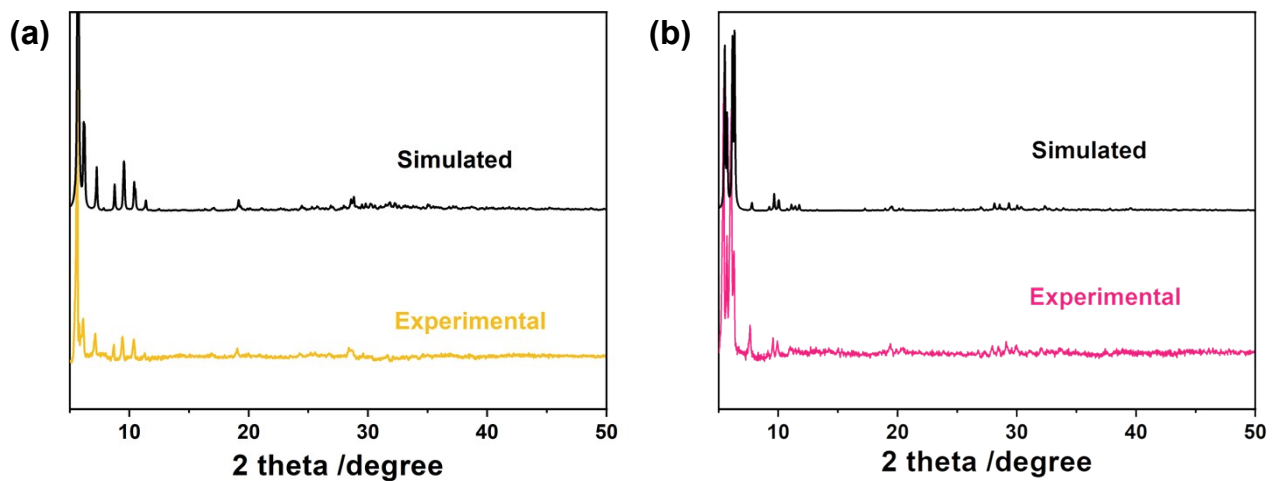


Fig. S4 Experimental and simulated PXRD patterns of (a) Ag₄₅ and (b) Ag₄₁ clusters.

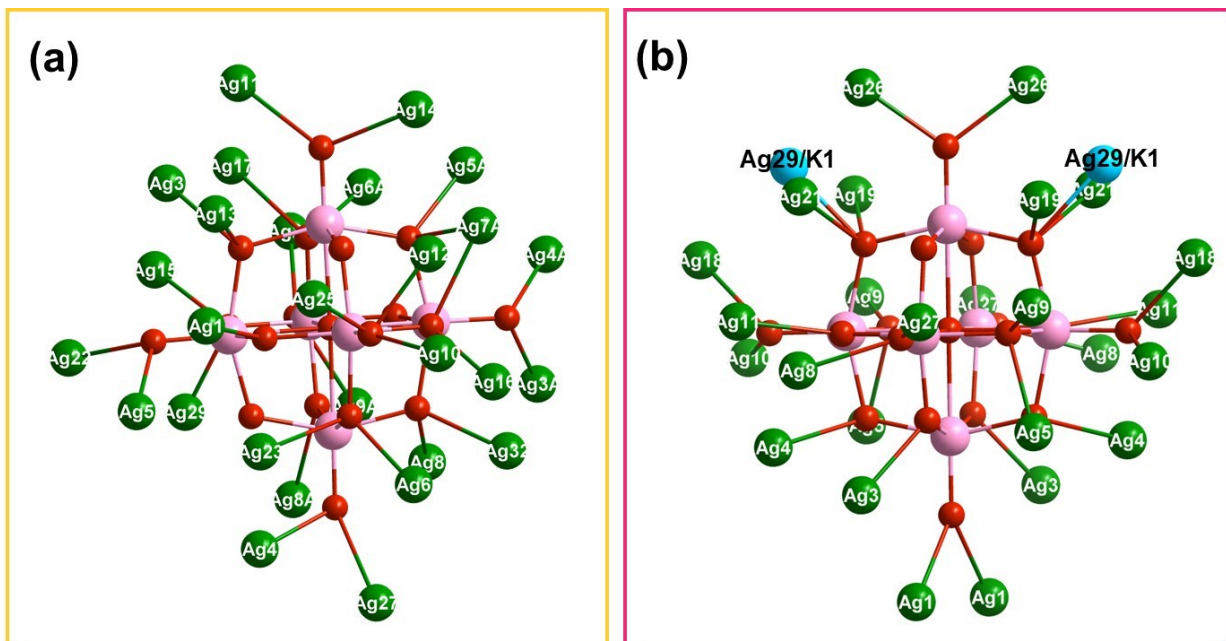


Fig. S5 The coordination modes of [Nb₆O₁₉]⁸⁻ anion towards 28 silver atoms in Ag₄₅ (a) and a total of 27 silver atoms in Ag₄₁ (b). Color codes: pink, Nb; green, Ag; red, O; sky blue, Ag/K. Note: in these two disordered Ag/K atoms, both Ag29 and K1 atoms were refined as 50% occupancy.

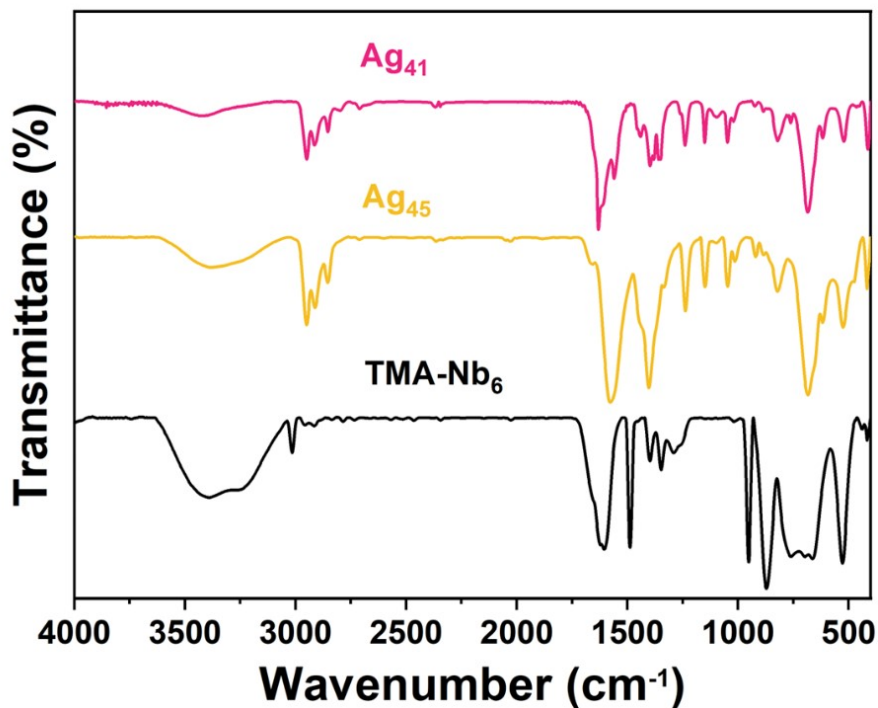


Fig. S6 FT-IR spectra of TBA-Nb₆, Ag₄₅, and Ag₄₁ clusters, respectively.

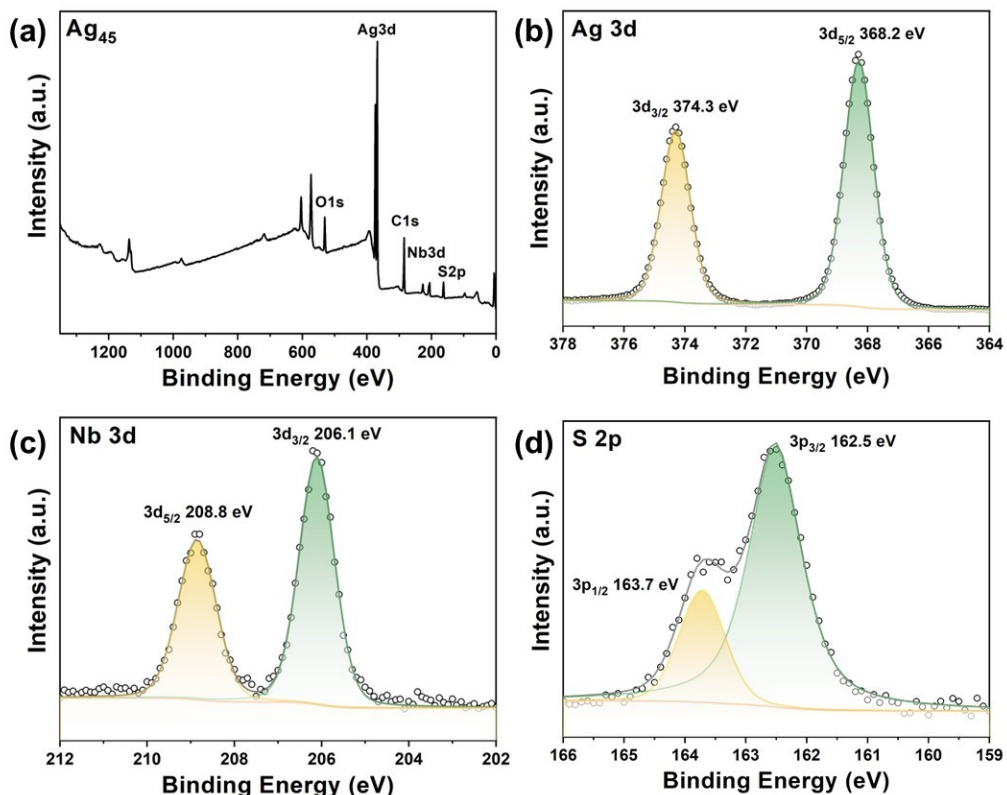


Fig. S7 (a) XPS survey spectrum of Ag₄₅ cluster; high resolution XPS spectra of (b) Ag 3d, (c) Nb 3d, and (d) S 2p in Ag₄₅ cluster.

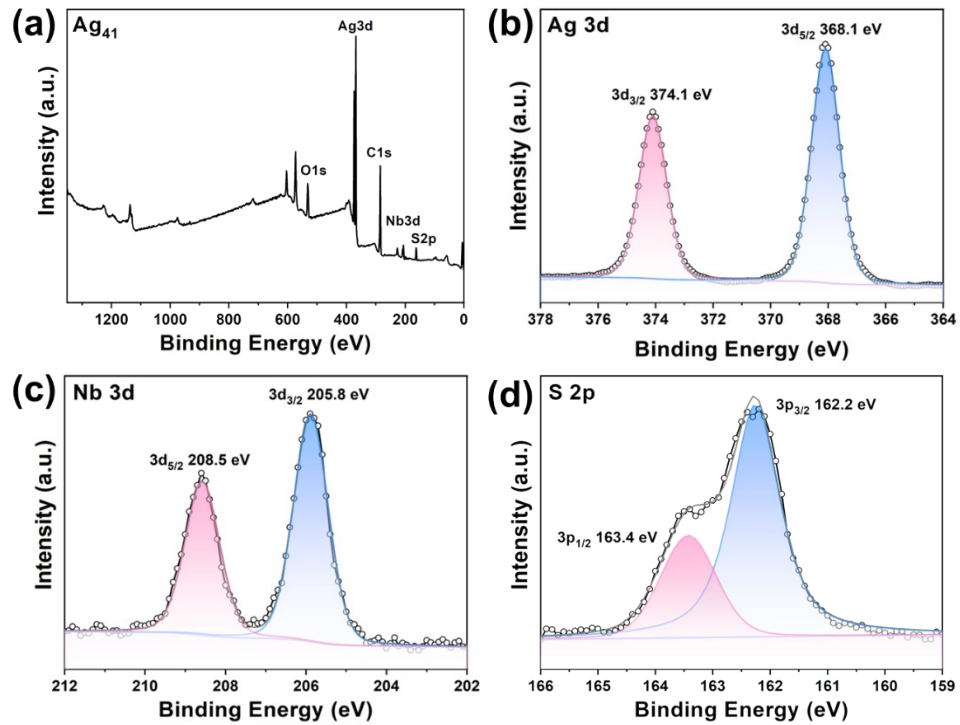
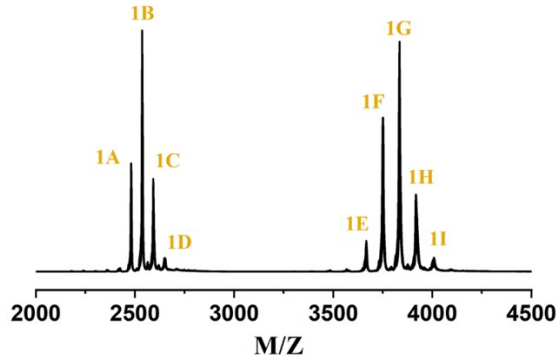
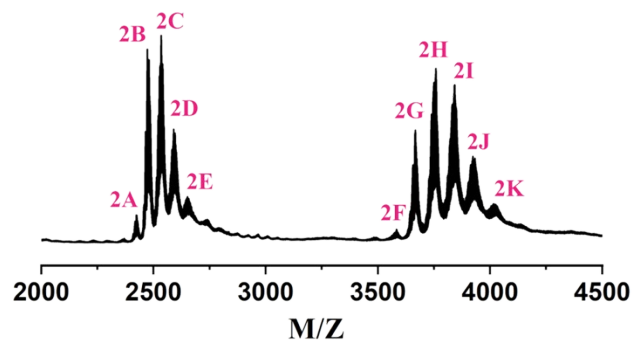


Fig. S8 (a) XPS survey spectrum of Ag_{41} cluster; high resolution XPS spectra of (b) Ag 3d, (c) Nb 3d, and (d) S 2p in Ag_{41} cluster.



Peak	Species	Exp. m/z	Sim. m/z
1A	$[\text{M} - 6\text{CH}_3\text{COO} - \text{iPrS} + \text{CH}_3\text{OH} - 4\text{Ag}]^{3+}$	2480.37	2480.58
1B	$[\text{M} - 5\text{CH}_3\text{COO} - \text{iPrS} + \text{CH}_3\text{OH} - 3\text{Ag}]^{3+}$	2536.38	2536.22
1C	$[\text{M} - 4\text{CH}_3\text{COO} - \text{iPrS} + \text{CH}_3\text{OH} - 2\text{Ag}]^{3+}$	2592.33	2591.85
1D	$[\text{M} - 3\text{CH}_3\text{COO} - \text{iPrS} + \text{CH}_3\text{OH} - \text{Ag}]^{3+}$	2648.03	2647.49
1E	$[\text{M} - 6\text{CH}_3\text{COO} - \text{iPrS} + \text{CH}_3\text{OH} - 5\text{Ag}]^{2+}$	3666.60	3666.94
1F	$[\text{M} - 5\text{CH}_3\text{COO} - \text{iPrS} + \text{CH}_3\text{OH} - 4\text{Ag}]^{2+}$	3750.01	3750.39
1G	$[\text{M} - 4\text{CH}_3\text{COO} - \text{iPrS} + \text{CH}_3\text{OH} - 3\text{Ag}]^{2+}$	3834.21	3833.85
1H	$[\text{M} - 3\text{CH}_3\text{COO} - \text{iPrS} + \text{CH}_3\text{OH} - 2\text{Ag}]^{2+}$	3916.90	3917.30
1I	$[\text{M} - 3\text{CH}_3\text{COO} + \text{CH}_3\text{OH} - \text{Ag}]^{2+}$	4007.61	4008.81

Fig. S9 Positive-ion ESI-MS spectrum and assigned formulae of Ag_{45} cluster dissolved in CH_3OH . Note: $\text{M} = [\text{Nb}_6\text{O}_{19}@\text{Ag}_{45}(\text{iPrS})_{23}(\text{CH}_3\text{COO})_{14}]$.



Peak	Species	Exp. m/z	Sim. m/z
2A	[M - 4CH ₃ COO - 2 <i>i</i> PrS + H ₂ O - Ag] ³⁺	2422.99	2422.71
2B	[M - 3CH ₃ COO - 2 <i>i</i> PrS + H ₂ O] ³⁺	2478.63	2478.34
2C	[M - 3CH ₃ COO - <i>i</i> PrS + Ag] ³⁺	2533.64	2533.35
2D	[M - 2CH ₃ COO - <i>i</i> PrS + 2Ag] ³⁺	2589.27	2588.99
2E	[M - CH ₃ COO - <i>i</i> PrS + H ₂ O + 3Ag] ³⁺	2650.91	2650.62
2F	[M - 4CH ₃ COO - 2 <i>i</i> PrS + H ₂ O - 2Ag] ²⁺	3580.56	3580.12
2G	[M - 3CH ₃ COO - 2 <i>i</i> PrS + CH ₃ OH - Ag] ²⁺	3671.03	3670.60
2H	[M - 2CH ₃ COO - 2 <i>i</i> PrS + CH ₃ OH] ²⁺	3754.46	3754.05
2I	[M - 2CH ₃ COO - <i>i</i> PrS + CH ₃ OH + Ag] ²⁺	3846.00	3845.56
2J	[M - CH ₃ COO - <i>i</i> PrS + CH ₃ OH + 2Ag] ²⁺	3929.45	3929.01
2K	[M - CH ₃ COO + CH ₃ OH + 3Ag] ²⁺	4020.96	4020.53

Fig. S10 Positive-ion ESI-MS spectrum and assigned formulae of Ag₄₁ cluster dissolved in CH₃OH. Note: M = (H₃O)₄[Nb₆O₁₉@Ag₄₁KS_{2.5}O₂(H₂O)_{7.5}(*i*PrS)₂₄(CH₃COO)₅].

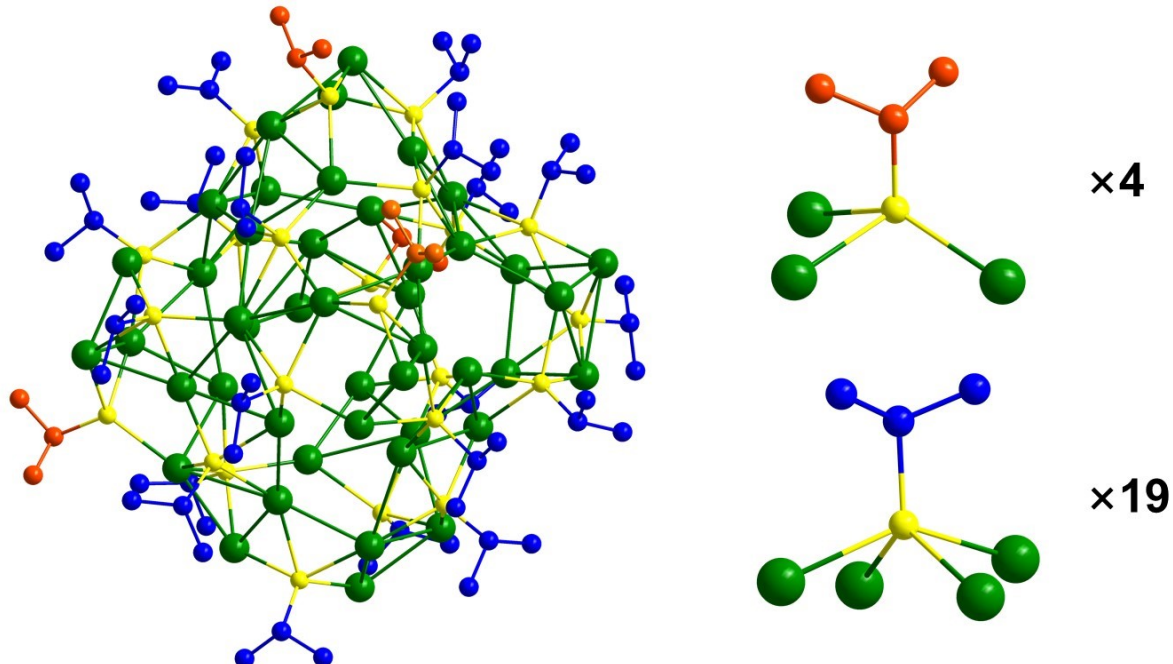


Fig. S11 The coordination modes of 23 *i*PrS⁻ ligands towards silver atoms in Ag₄₅ cluster. Color codes: green, Ag; yellow, S; orange, C; blue, C.

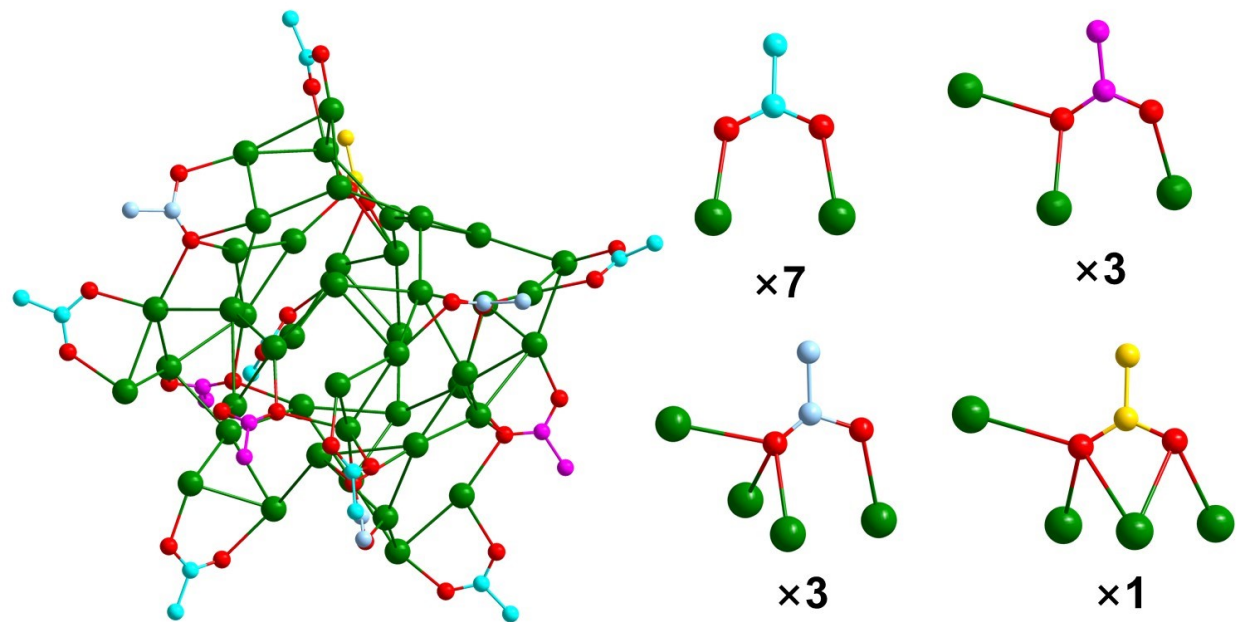


Fig. S12 The coordination modes of 14 CH_3COO^- ligands towards silver atoms in Ag_{45} cluster. Color codes: green, Ag; red, O; turquoise, C; pink, C; light turquoise, C; gold, C.

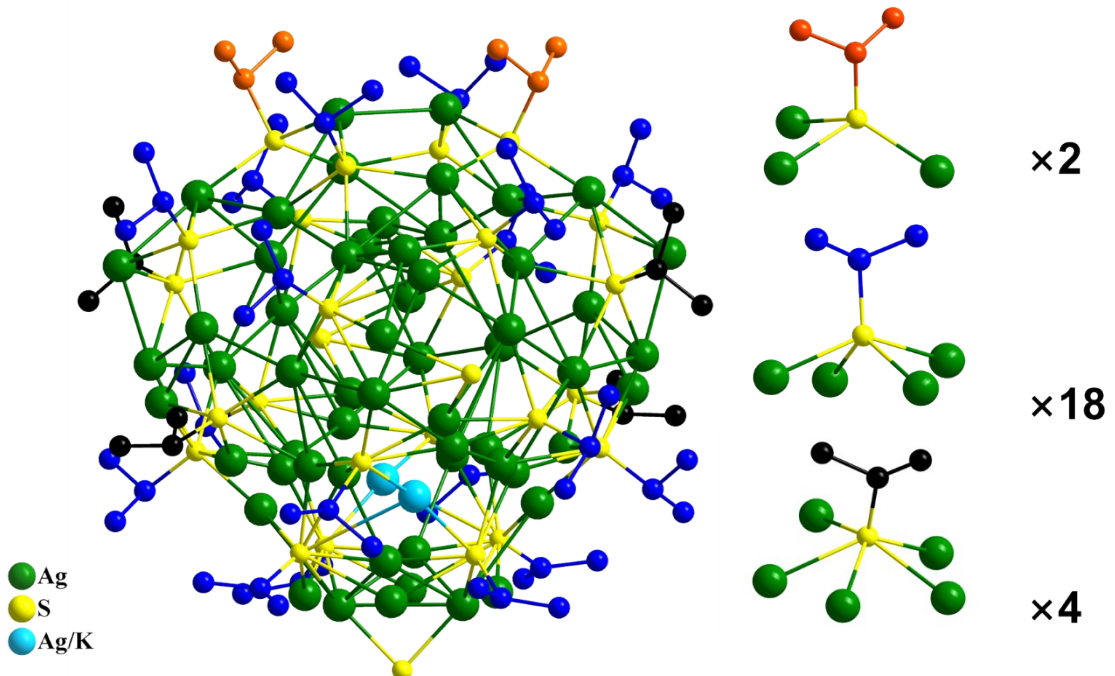


Fig. S13 The coordination modes of 24 $i\text{PrS}^-$ ligands towards silver atoms in Ag_{41} cluster. Color codes: green, Ag; yellow, S; black, C; orange, C; blue, C; sky blue, Ag/K.

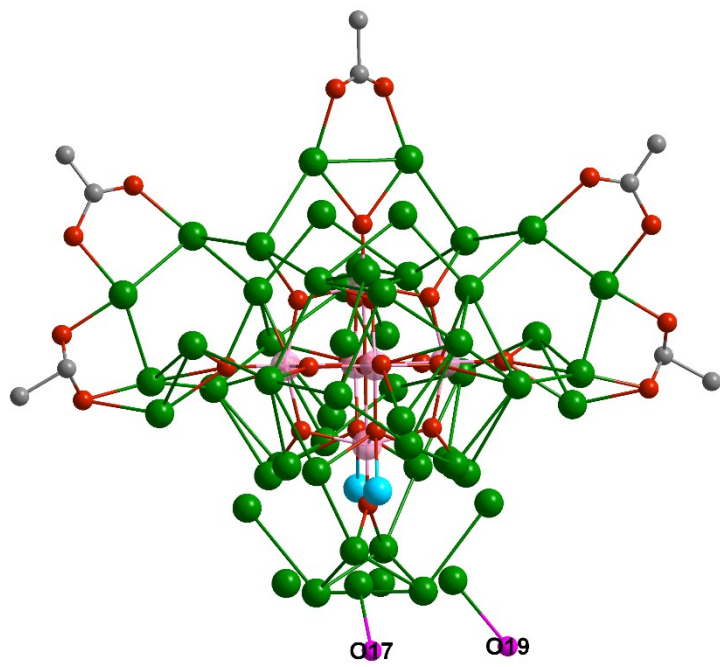


Fig. S14 The coordination modes of $5 \text{CH}_3\text{COO}^-$ ligands towards silver atoms in Ag_{41} cluster. Color codes: green, Ag; pink, Nb; red, O; purple, O; gray, C; sky blue, Ag/K.

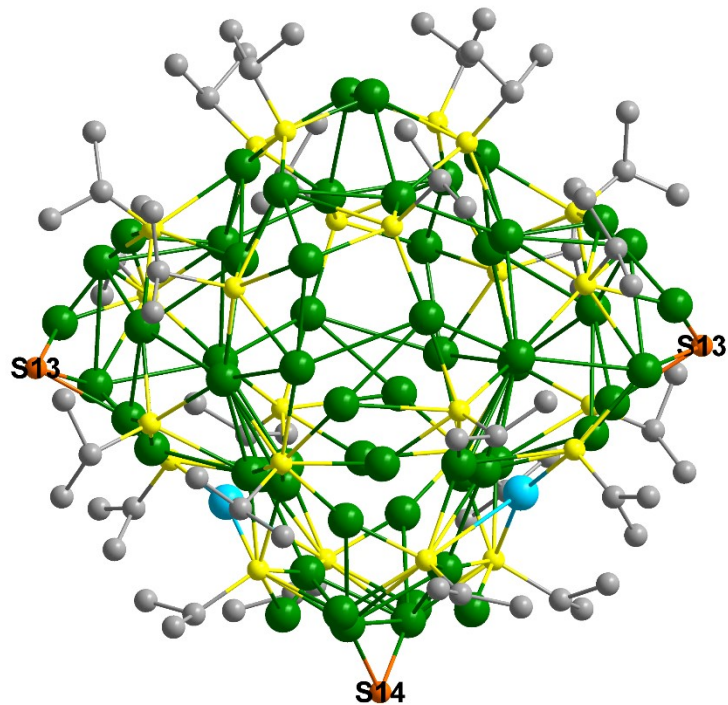


Fig. S15 The coordination modes of S atoms in Ag_{41} cluster. Color codes: green, Ag; yellow, S; orange, S; gray, C; sky blue, K/Ag. Note: The S14 atom adopted 50% occupancy (Occu: 1; Xtal: 0.25).

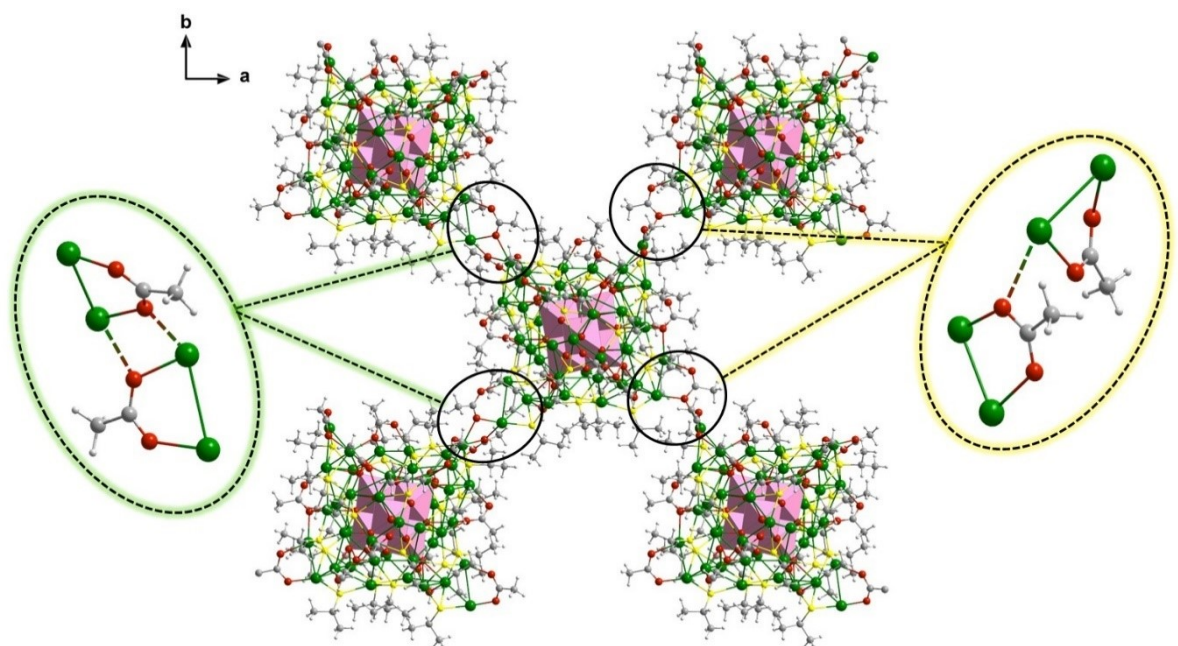


Fig. S16 Packing structure of Ag_{45} cluster in the bc plane. Color codes: green, Ag; pink polyhedron, $[\text{Nb}_6\text{O}_{19}]^{8-}$; yellow, S; red, O; gray, C; white, H.

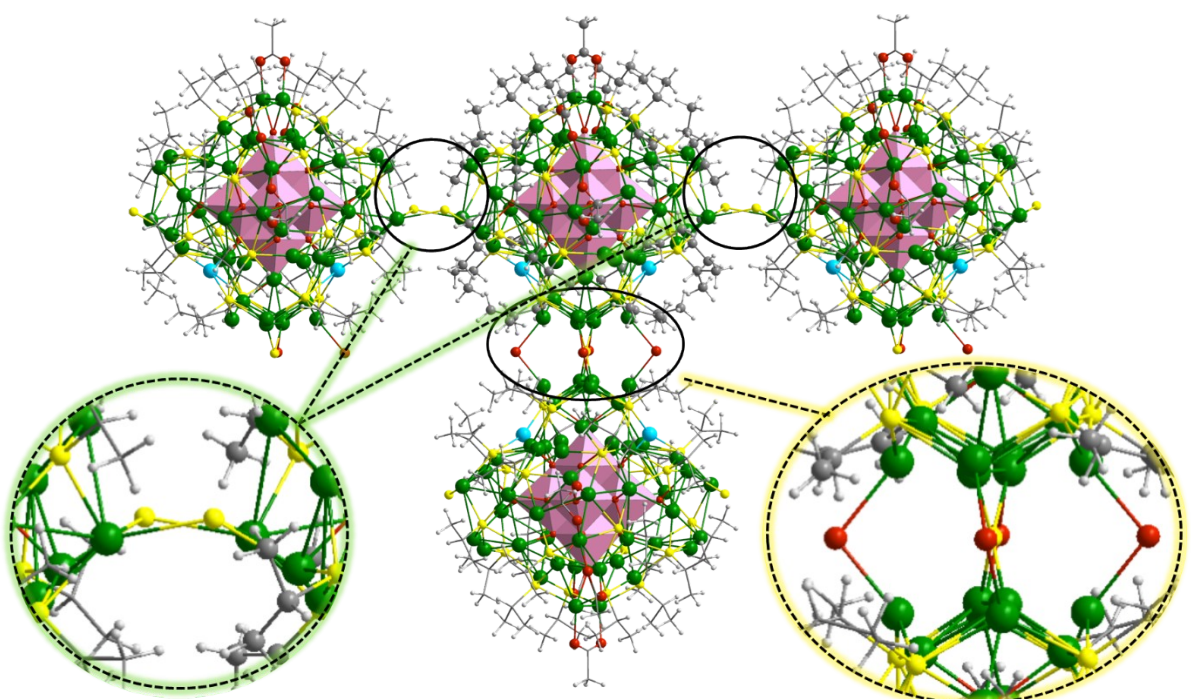


Fig. S17 Packing structure of Ag_{41} cluster. Color codes: green, Ag; pink polyhedron, $[\text{Nb}_6\text{O}_{19}]^{8-}$; yellow, S; red, O; gray, C; white, H; sky blue, Ag/K.

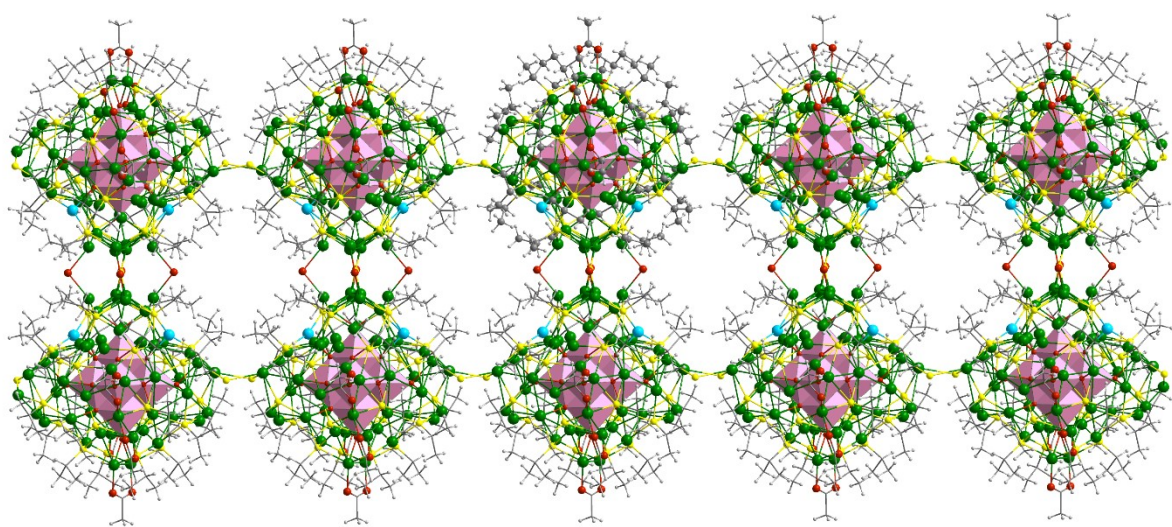


Fig. S18 One-dimensional chain structure of Ag_{41} cluster. Color codes: green, Ag; pink polyhedron, $[\text{Nb}_6\text{O}_{19}]^{8-}$; yellow, S; red, O; gray, C; white, H; sky blue, Ag/K.

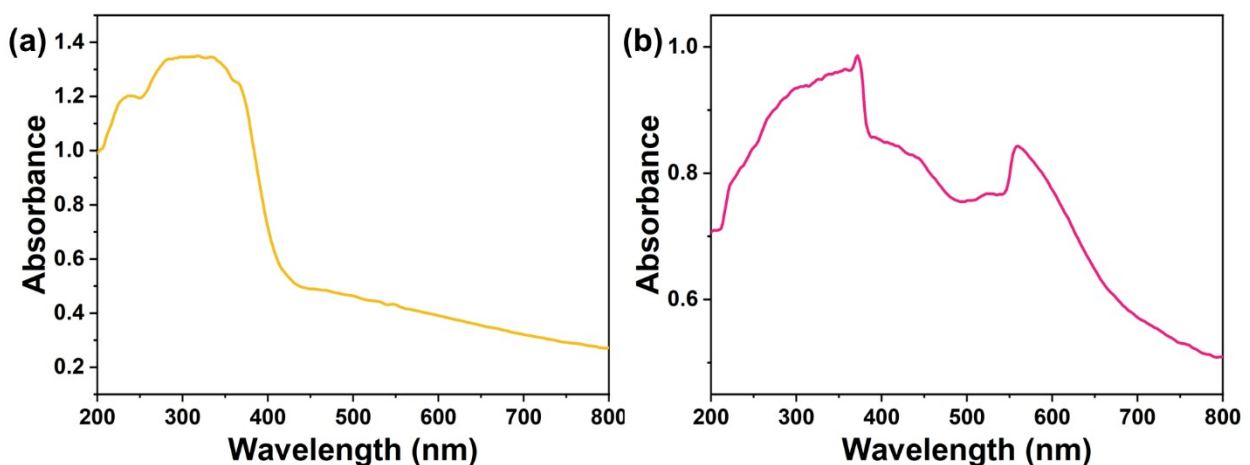


Fig. S19 The solid-state UV–vis diffuse reflectance spectra of (a) Ag_{45} and (b) Ag_{41} clusters collected by using optional Integration Sphere accessory.

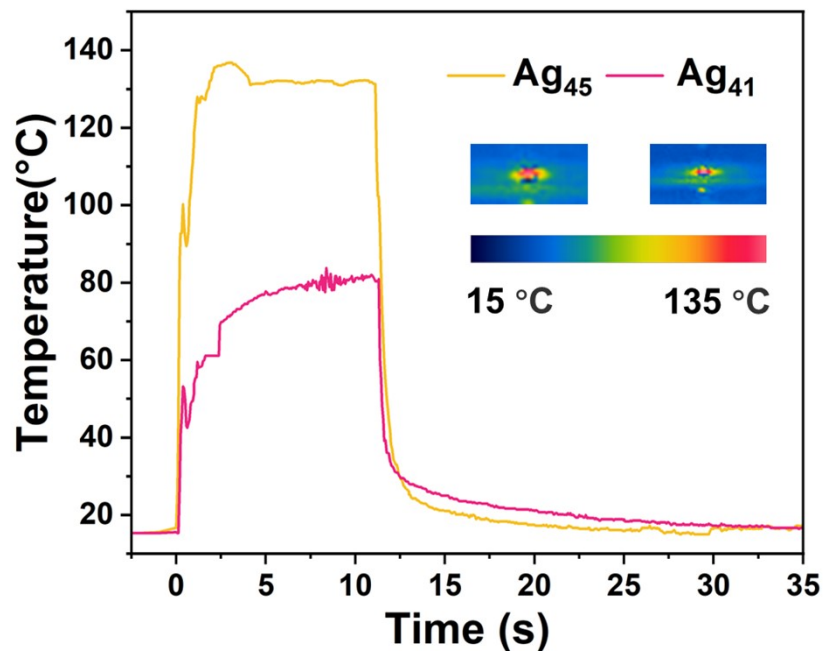


Fig. S20 Photothermal conversion of Ag_{45} and Ag_{41} clusters under 532 nm laser irradiation (1.0 W cm^{-2}). Insets: thermal images of Ag_{45} and Ag_{41} clusters at the highest temperature.

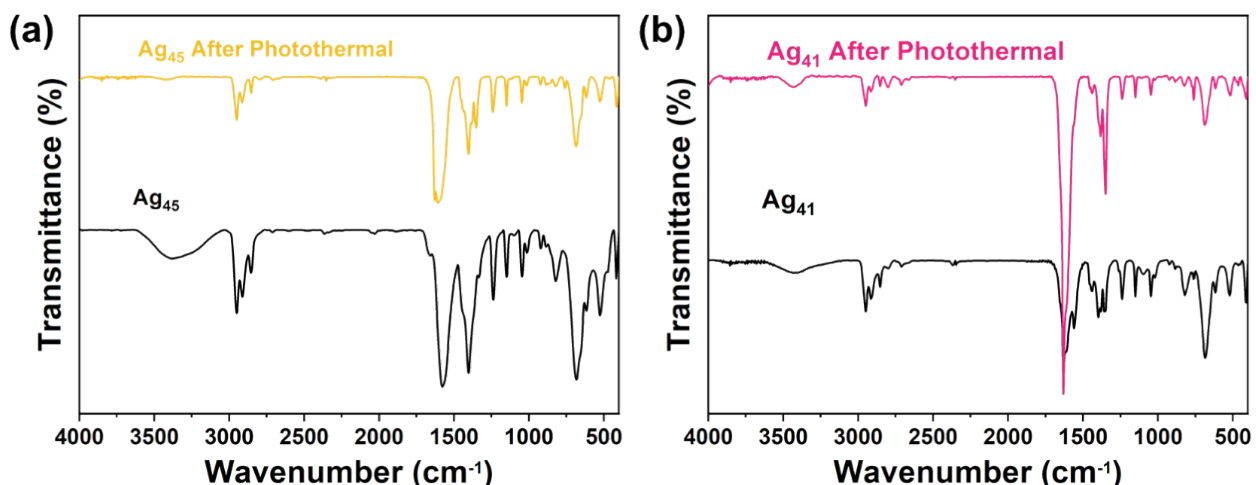


Fig. S21 FT-IR spectra of (a) Ag_{45} and (b) Ag_{41} clusters before and after photothermal tests.

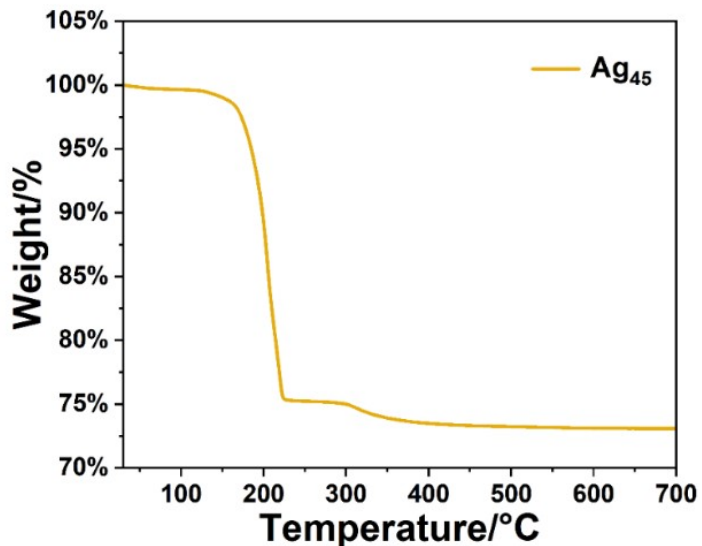


Figure S22. TGA curves of Ag_{45} at a scanning rate of 10 °C/min under N_2 atmosphere. Note: The structure remains stable at a temperature up to 150 °C, and the further increase of temperature to 700 °C led to a weight loss of ~27.5%, corresponding to the partial loss of the peripheral organic ligands. The final residue should be a mixture of Nb_2O_5 and Ag_2S species.

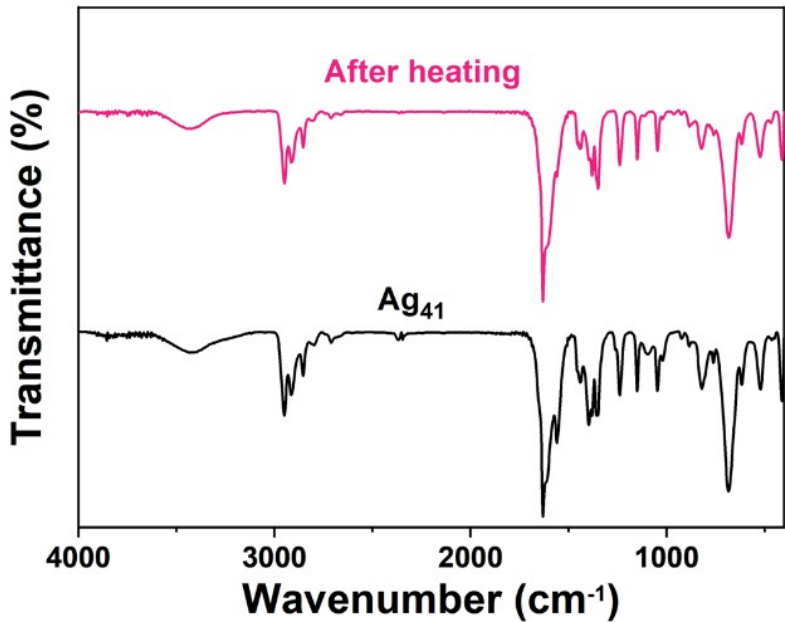


Figure S23. FT-IR spectra of Ag_{41} clusters before and after heating at 80 °C for 10 minutes. Note: the unchanged FT-IR spectra confirmed its thermal stability which is also consistent with the FT-IR results collected after the photothermal test.

Table 1. Crystal data and structure refinements for **Ag₄₅** and **Ag₄₁**.

Compound	Ag ₄₅	Ag ₄₁
Empirical formula	C ₉₇ H ₂₀₃ Ag ₄₅ Nb ₆ O ₄₇ S ₂₃	C ₈₂ H ₂₁₀ Ag ₄₁ KNb ₆ O _{42.5} S _{26.5}
M _r (g mol ⁻¹)	8270.57	7745.31
Temperature/K	179.99	179.99
Crystal system	orthorhombic	tetragonal
Space group	Pbca	P4 ₂ 2 ₁ 2
a (Å)	28.7435(6)	32.1512(5)
b (Å)	28.3372(6)	32.1512(5)
c (Å)	48.7703(2)	17.6732(3)
α (°)	90.00	90.00
β (°)	90.00	90.00
γ (°)	90.00	90.00
V/Å ³	39723.9(2)	18268.8(6)
Z	8	4
ρ _{calcd} (g cm ⁻³)	2.766	2.816
μ mm ⁻¹	4.946	5.017
F(000)	31120	14632
Crystal size/mm ³	0.21 × 0.2 × 0.19	0.3 × 0.3 × 0.2
limiting indices	−33 ≤ h ≤ 34 −32 ≤ k ≤ 33 −25 ≤ l ≤ 58	−43 ≤ h ≤ 24 −33 ≤ k ≤ 40 −22 ≤ l ≤ 22
no. of reflections collected	139769	77451
no. of independent reflections	34941	22246
restraints/parameters	1895/2098	314/796
θ _{min} /θ _{max}	1.951/25.000	2.003/30.141
R _{int}	0.1186	0.0573
GooF	1.033	1.074
R [I > 2σ]	R ₁ = 0.0761 wR ₂ = 0.1835	R ₁ = 0.0800 wR ₂ = 0.2074
R(all data)	R ₁ = 0.1290 wR ₂ = 0.2071	R ₁ = 0.1399 wR ₂ = 0.2356
$R_1 = \sum(F_o - F_c)/\sum F_o $, $wR_2 = \{\sum[\mathbf{w}(F_{\circ}^2 - F_{\circ}^2)^2]/\sum[\mathbf{w}(F_{\circ}^2)^2]\}^{1/2}$		

Table S2. Selected bond distances (Å) for **Ag₄₅**.

Ag10	Ag25	3.135(2)	Ag33	S6	2.516(4)
Ag10	Ag9	2.851(2)	Ag33	S9	2.607(5)
Ag10	Ag30	2.8424(2)	Ag34	Ag19	3.104(2)
Ag10	Ag12	2.9440(2)	Ag34	S8	2.412(6)
Ag10	S10	2.470(4)	Ag34	O1	2.152(2)
Ag10	S14	2.490(5)	Ag35	Ag2	2.850(2)
Ag10	O11	2.414(1)	Ag35	S18	2.563(5)
Ag11	S6	2.485(5)	Ag35	S11	2.553(5)
Ag11	S18	2.503(5)	Ag35	O47	2.427(1)
Ag11	O12	2.336(1)	Ag35	O45	2.335(1)
Ag12	S9	2.461(4)	Ag36	Ag6A	3.174(3)
Ag12	O39	2.317(1)	Ag36	S21	2.571(4)
Ag12	O11	2.521(1)	Ag36	S22	2.577(4)
Ag13	Ag33	2.986(2)	Ag36	S8	2.529(5)
Ag13	Ag11	3.306(2)	Ag36	Ag9A	2.982(1)
Ag13	S2	2.450(4)	Ag37	S12	2.429(4)
Ag13	O16	2.301(1)	Ag37	S17	2.897(5)
Ag13	Ag1	3.0733(1)	Ag37	O22	2.188(1)
Ag13	O29	2.299(1)	Ag3A	S4	2.619(9)
Ag14	Ag7A	3.129(6)	Ag3A	O44	2.585(2)
Ag14	Ag2	3.138(2)	Ag4	Ag21	2.938(2)
Ag14	S9	2.420(4)	Ag4	Ag23	3.3122(2)
Ag14	O41	2.513(1)	Ag4	Ag27	2.9616(2)
Ag14	S11	2.400(4)	Ag4	Ag7	3.277(2)
Ag14	Ag5A	3.154(1)	Ag4	S24	2.439(5)
Ag15	Ag22	3.328(2)	Ag4A	Ag3A	2.938(1)
Ag15	Ag29	3.3712(2)	Ag4A	S4	2.359(7)
Ag15	Ag17	2.987(2)	Ag4A	Ag5A	3.095(1)
Ag15	S1	2.538(5)	Ag4A	Ag1A	3.314(1)
Ag15	S3	2.538(5)	Ag5	Ag23	3.089(2)
Ag15	O42	2.383(1)	Ag5	Ag37	3.003(2)
Ag16	Ag32	3.061(2)	Ag5	S24	2.404(4)
Ag16	S10	2.535(4)	Ag5	S17	2.436(4)
Ag16	S5	2.548(5)	Ag5	O33	2.470(9)
Ag16	O28	2.351(9)	Ag5	Ag1	3.0016(2)
Ag16	O24	2.585(1)	Ag6	Ag16	2.9990(2)
Ag17	Ag6A	3.131(3)	Ag6	Ag32	3.306(2)
Ag17	S1	2.439(5)	Ag6	Ag27	3.2848(2)
Ag17	S18	2.480(5)	Ag6	S13	2.512(4)
Ag17	O8	2.595(9)	Ag6	S10	2.574(4)
Ag19	S1	2.742(5)	Ag6	O25	2.320(9)
Ag19	O26	2.573(1)	Ag6	O3	2.417(1)
Ag19	O37	2.321(1)	Ag6A	S21	2.483(5)
Ag19	O19	2.495(1)	Ag6A	O8	2.284(1)
Ag19	O20	2.554(2)	Ag6A	O47	2.292(1)
Ag2	Ag11	3.025(2)	Ag7	Ag29	3.276(2)
Ag2	S6	2.431(5)	Ag7	S24	2.631(5)

Ag2	S11	2.923(5)	Ag7	S12	2.585(5)
Ag2	O40	2.218(1)	Ag7	S20	2.615(5)
Ag20	Ag34	3.062(2)	Ag7	O6	2.483(1)
Ag20	Ag36	3.262(2)	Ag7A	Ag31	3.163(7)
Ag20	Ag19	3.080(2)	Ag7A	Ag12	2.967(5)
Ag20	Ag6A	3.253(3)	Ag7A	S9	2.622(8)
Ag20	S1	2.453(5)	Ag7A	O13	2.582(1)
Ag20	S8	2.440(5)	Ag7A	O28	2.539(1)
Ag20	O48	2.551(1)	Ag7A	S7	2.521(7)
Ag21	Ag7	2.995(2)	Ag7A	Ag5A	3.354(8)
Ag21	S19	2.454(4)	Ag8	Ag26	3.0963(2)
Ag21	S20	2.508(4)	Ag8	S15	2.543(4)
Ag21	O43	2.236(1)	Ag8	O27	2.443(1)
Ag22	Ag37	2.977(2)	Ag8	Ag3A	3.124(7)
Ag22	Ag29	3.271(2)	Ag8	Ag8A	3.295(4)
Ag22	S12	2.459(5)	Ag8	Ag9A	3.104(1)
Ag22	S3	2.517(5)	Ag8A	O5	2.318(2)
Ag22	O33	2.571(1)	Ag8A	Ag9A	2.96(2)
Ag22	O7	2.405(2)	Ag9	Ag30	3.367(2)
Ag23	S24	2.573(5)	Ag9	S16	2.501(5)
Ag23	S16	2.528(4)	Ag9	S10	2.539(5)
Ag23	Ag1	3.2773(2)	Ag9	O15	2.288(1)
Ag23	O3	2.488(1)	Nb1	O16	2.044(9)
Ag24	Ag37	2.908(2)	Nb1	O35	1.997(1)
Ag24	S17	2.574(4)	Nb1	O42	2.036(1)
Ag24	S3	2.539(5)	Nb1	O38	2.399(1)
Ag24	O31	2.305(2)	Nb1	O33	1.789(1)
Ag24	O29	2.479(1)	Nb1	O18	1.970(9)
Ag25	Ag12	3.279(3)	Nb2	O8	2.007(9)
Ag25	S2	2.513(4)	Nb2	O42	2.023(1)
Ag25	S16	2.663(4)	Nb2	O36	1.953(1)
Ag25	O39	2.501(1)	Nb2	O38	2.360(9)
Ag25	S14	2.484(4)	Nb2	O26	1.787(1)
Ag25	Ag1	3.090(2)	Nb2	O34	1.984(9)
Ag26	Ag27	3.155(2)	Nb3	O41	1.774(9)
Ag26	Ag28	2.944(2)	Nb3	O16	2.029(1)
Ag26	S13	2.496(4)	Nb3	O8	2.034(1)
Ag26	S15	2.521(4)	Nb3	O4	1.972(9)
Ag26	O17	2.314(1)	Nb3	O13	2.011(1)
Ag27	Ag28	3.155(2)	Nb3	O38	2.385(9)
Ag27	S13	2.454(5)	Nb4	O38	2.383(9)
Ag27	S19	2.495(5)	Nb4	O25	2.019(1)
Ag27	O14	2.410(1)	Nb4	O27	2.032(1)
Ag28	S15	2.552(4)	Nb4	O30	1.776(9)
Ag28	S19	2.516(5)	Nb4	O34	2.003(9)
Ag28	O46	2.449(1)	Nb4	O18	1.955(1)
Ag28	O32	2.388(1)	Nb5	O4	1.957(9)
Ag29	S20	2.435(4)	Nb5	O39	1.805(9)
Ag29	O42	2.300(1)	Nb5	O28	2.016(1)

Ag29	O20	2.384(1)	Nb5	O35	1.998(1)
Ag2A	S5	2.483(7)	Nb5	O38	2.372(9)
Ag2A	Ag3A	3.062(2)	Nb5	O25	2.001(1)
Ag2A	S4	2.519(7)	Nb6	O23	1.811(1)
Ag2A	O10	2.437(2)	Nb6	O13	2.017(9)
Ag2A	Ag1A	3.269(1)	Nb6	O28	2.035(9)
Ag3	Ag15	3.0033(2)	Nb6	O36	1.958(1)
Ag3	Ag13	3.2305(2)	Nb6	O38	2.372(1)
Ag3	Ag17	2.9101(2)	Nb6	O27	2.024(9)
Ag3	Ag11	3.302(2)	O13	Ag5A	2.400(1)
Ag3	S18	2.528(5)	O19	O5	1.77(2)
Ag3	O16	2.418(9)	O19	Ag9A	2.295(2)
Ag3	S3	2.521(5)	O21	Ag1A	2.322(2)
Ag30	S14	2.377(4)	O23	Ag4A	2.563(1)
Ag30	O46	2.214(1)	O23	Ag3A	2.410(1)
Ag30	O32	2.351(1)	O35	Ag1	2.403(1)
Ag31	Ag2A	3.307(5)	S11	Ag5A	2.706(1)
Ag31	S5	2.558(4)	S15	Ag8A	2.657(8)
Ag31	S7	2.575(5)	S16	Ag1	2.650(4)
Ag31	O2	2.300(2)	S17	Ag1	2.538(5)
Ag31	Ag1A	2.865(5)	S2	Ag1	2.759(4)
Ag32	S13	2.542(4)	S22	Ag3A	2.650(1)
Ag32	S5	2.517(5)	S22	Ag9A	2.348(1)
Ag32	O27	2.434(1)	S4	Ag1A	2.539(7)
Ag33	Ag11	3.310(2)	S7	Ag1A	2.574(1)
Ag33	S2	2.476(4)			

Table S3. Selected bond distances (Å) for Ag₄₁.

Ag1	S2	2.515(6)	Nb2	O8	1.992(1)
Ag1	S1 ¹	2.594(6)	Nb2	O2	2.002(1)
Ag1	O1	2.435(1)	Nb2	O5	2.004(1)
Ag1	O12	2.26(2)	Nb2	O7	2.377(1)
Ag10	S3	2.422(6)	Nb2	O4	1.789(1)
Ag10	S7	2.457(8)	Nb2	O9 ¹	1.970(1)
Ag10	O4	2.503(1)	Nb3	O3 ¹	1.974(1)
Ag7	Ag27	2.749(6)	Nb3	O10	1.979(1)
Ag26	Ag30	2.760(2)	Nb3	O6	1.751(1)
Ag26	Ag30 ¹	2.770(3)	Nb3	O5	1.981(1)
Ag6	Ag7	2.884(4)	Nb3	O7	2.374(2)
Ag11	S4	2.464(6)	Nb3	O9	1.998(1)
Ag11	S12 ¹	2.494(6)	Nb4	O10	2.008(1)
Ag11	O9 ¹	2.499(1)	Nb4	O10 ¹	2.008(1)
Ag16	Ag14	2.909(9)	Nb4	O8 ¹	2.007(1)
Ag26	Ag21	2.920(2)	Nb4	O8	2.007(1)
Ag9	Ag27	2.947(9)	Nb4	O7	2.377(1)
Ag12	O19	2.566(2)	Nb4	O11	1.760(2)
Ag5	Ag6	2.956(4)	O10	Ag20	2.450(1)

Ag10	Ag18	2.962(6)	O11	Ag26 ¹	2.291(2)
Ag2	Ag5	2.968(3)	O11	Ag26	2.291(2)
Ag8	Ag28	2.985(6)	O17	Ag25 ³	2.514(2)
Ag19	S7	2.714(9)	O17	Ag25	2.514(2)
Ag19	S11	2.442(1)	O4	Ag18	2.379(1)
Ag19	O8	2.581(1)	O6	Ag27	2.419(1)
Ag3	Ag4	2.991(4)	O6	Ag28	2.423(2)
Ag8	Ag11 ¹	3.002(3)	O8	Ag21	2.407(2)
Ag9	Ag19	3.029(7)	O8	Ag29	2.406(1)
Ag2	S2	2.504(6)	O8	K1	2.406(1)
Ag2	S1	2.539(6)	S10	Ag25	2.694(1)
Ag2	S3	2.696(6)	S10	Ag26	2.222(1)
Ag10	Ag5	3.041(4)	S10	Ag22	2.460(1)
Ag11	Ag22	3.082(6)	S10	Ag21	2.699(1)
Ag10	Ag13	3.085(5)	S10	Ag12 ¹	2.526(8)
Ag1	Ag1 ¹	3.088(4)	S10	Ag23	2.232(1)
Ag19	Ag17	3.089(1)	S10	K1	3.711(1)
Ag1	Ag3 ¹	3.092(3)	S10	Ag30 ¹	2.910(2)
Ag27	O16	2.160(3)	S11	Ag20	2.512(1)
Ag28	O16	2.340(5)	S11	Ag25	2.477(9)
Ag15	Ag17	3.159(1)	S11	Ag26	2.402(9)
Ag9	Ag5	3.160(4)	S11	Ag12	2.491(9)
Ag3	S1	2.521(6)	S11	Ag29	2.520(9)
Ag3	S6 ¹	2.453(7)	S11	K1	2.520(9)
Ag3	O3	2.373(1)	S11	Ag30	2.540(2)
Ag3	Ag61	3.172(4)	S12	Ag28	2.941(2)
Ag4	S4	2.462(5)	S12	Ag221	2.786(1)
Ag4	S1	2.469(6)	S12	Ag24 ¹	2.423(7)
Ag4	O2	2.518(1)	S13	Ag15	2.698(1)
Ag9	Ag20	3.202(1)	S13	Ag15 ²	2.916(1)
Ag10	Ag9	3.222(3)	S13	Ag16 ²	2.458(8)
Ag4	Ag13	3.237(7)	S13	Ag16	2.513(1)
Ag5	S3	2.662(6)	S13	Ag18	2.577(2)
Ag5	S5	2.620(7)	S14	Ag30	2.350(2)
Ag5	O5	2.517(1)	S14	Ag30 ³	2.350(2)
Ag6	S2	2.472(6)	S14	Ag30 ¹	2.350(2)
Ag6	S5	2.634(7)	S14	Ag30 ⁴	2.350(2)
Ag6	O13	2.310(3)	S3	Ag13	2.530(7)
Ag30	Ag30 ¹	3.250(5)	S3	Ag14	2.426(7)
Ag23	Ag30 ¹	3.280(2)	S4	Ag15	2.655(7)
Ag7	O14	2.320(3)	S4	Ag16	2.375(7)
Ag7	O15	2.170(3)	S4	Ag13	2.649(7)
Ag11	Ag21	3.302(2)	S4	Ag14	2.465(7)
Ag8	S12	2.394(6)	S5	Ag7	2.690(8)
Ag8	S6	2.365(7)	S5	Ag27	2.668(1)
Ag8	O6	2.494(1)	S6	Ag7	2.581(8)
Ag11	Ag4	3.305(3)	S7	Ag17	2.365(9)
Ag15	Ag13	3.346(7)	S7	Ag18	2.666(1)
Ag2	Ag4	3.348(3)	S8	Ag22	2.880(2)

Ag9	S9 ¹	2.656(7)	S8	Ag21	2.253(1)
Ag9	S7	2.576(6)	S8	Ag15	2.557(9)
Ag9	S5	2.567(7)	S8	Ag17	2.377(1)
Ag9	O5	2.563(1)	S8	Ag18	2.436(9)
Ag10	Ag17	3.359(9)	S8	Ag29	2.434(9)
Ag11	Ag15	3.371(5)	S8	K1	2.434(9)
Nb1	O3	2.002(1)	S9	Ag20 ¹	2.383(9)
Nb1	O3 ¹	2.002(1)	S9	Ag27 ¹	2.703(9)
Nb1	O1	1.781(2)	S9	Ag28 ¹	2.428(1)
Nb1	O2	1.993(1)	S9	Ag24	2.455(7)
Nb1	O2 ¹	1.993(1)	S9	Ag23	2.468(8)
Nb1	O7	2.374(1)			

(Symmetric codes: ¹ + *y*, + *x*, 1 - *z*; ² + *y*, + *x*, *z*; ³ 1-*y*, 1-*x*, 1 - *z*; ⁴ 1 - *x*, 1 - *y*, +*z*)

Table S4. BVS values for Nb atoms of Ag₄₅.

Nb1	4.84	Nb4	4.87
Nb2	4.88	Nb5	4.80
Nb3	4.71	Nb6	4.77

Table S5. BVS values for Nb atoms of Ag₄₁.

Nb1	4.87	Nb3	5.12
Nb2	4.89	Nb4	4.87

Table S6. PL decay lifetimes of Ag₄₅ and Ag₄₁ clusters upon excitation at 390 nm.

Compounds	τ_1 (μs)	τ_2 (μs)	τ_3 (μs)	τ_{ave} (μs)
Ag ₄₅	1.98	19.41	80.10	5.27
Ag ₄₁	6.64	24.77	89.84	27.39

References

1. Z. Wang, H.-F. Su, X.-P. Wang, Q.-Q. Zhao, C.-H. Tung, D. Sun and L.-S. Zheng, *Chem. Eur. J.*, 2018, **24**, 1640-1650.
2. L. B. Fullmer, R. H. Mansergh, L. N. Zakharov, D. A. Keszler and M. Nyman, *Cryst. Growth Des.*, 2015, **15**, 3885-3892.
3. O. V. Dolomanov, L. J. Bourhis, R. J. Gildea, J. A. K. Howard and H. Puschmann, *J. Appl. Crystallogr.*, 2009, **42**, 339-341.
4. L. J. Bourhis, O. V. Dolomanov, R. J. Gildea, J. A. K. Howard and H. Puschmann, *Acta Crystallogr. A*, 2015, **71**, 59-75.
5. G. Sheldrick, *Acta Crystallogr. A*, 2008, **64**, 112-122.
6. G. Sheldrick, *Acta Crystallogr. C*, 2015, **71**, 3-8.
7. N. E. Brese and M. O'Keeffe, *Acta Crystallogr. B*, 1991, **47**, 192-197.